# Quantitative Comparison of Kinetic Stabilities of Metallomacrocycle-Based Rotaxanes

**Sung-Youn Chang, Hye-Young Jang, and Kyu-Sung Jeong*[a]**

**Abstract:** Four mononuclear metallomacrocycles with identical cavities but different transition metals ($Os^{VI}$, $Pd^{II}$, $Pt^{II}$, and $Re^{I}$) were prepared. With these metallomacrocycles, the corresponding rotaxanes **2-Os**, **2-Pd**, **2-Pt**, and **2-Re** were self-assembled by hydrogen-bonding interactions. The kinetic stabilities of the rotaxanes were determined quantitatively and compared with each other by $^1$H NMR spectroscopic techniques, including two-dimensional exchange spectroscopy (2D-EXSY) experiments. The activation free energies ($\Delta G^{\neq}$) for the exchange between the rotaxanes **2-Os**, **2-Pd** and **2-Pt** and their free components were determined to be 15.5, 16.0, and 16.4 kcal mol$^{-1}$, respectively. These magnitudes imply that the rotaxanes **2-Os**, **2-Pd** and **2-Pt** are kinetically labile at room temperature and exist only as equilibrium mixtures with free components in solution. In contrast, the rotaxane **2-Re** is kinetically stable enough to be isolated in pure form by silica gel chromatography under ordinary laboratory conditions. However, at higher temperatures ($>60\,^{\circ}$C) **2-Re** was slowly disassembled into its components until the equilibrium was established. The rate constants were measured at three different temperatures, and the Eyring plot yielded the activation enthalpy $\Delta H^{\neq} = 35$ kcal mol$^{-1}$ and the activation entropy $\Delta S^{\neq} = 27$ eu for the disassembly of the rotaxane **2-Re** in $Cl_2CDCDCl_2$. These thermodynamic parameters gave the activation free energy $\Delta G^{\neq}_{\mathrm{off}} = 27.1$ kcal mol$^{-1}$ at 25 °C. Consequently, **2-Re** is one example of a novel metallomacrocycle-based rotaxane that contains a coordination bond with enough strength to allow both for isolation in pure form around room temperature and for self-assembly at higher temperatures.

**Keywords:** kinetic stability · metallomacrocycles · rotaxanes · self-assembly

## Introduction

Mechanically interlocked molecules have become popular synthetic targets in supramolecular chemistry in recent years; this is in part because of their potential applications as molecular switches, motors, and devices.[1, 2] Rotaxanes are typical examples of such supermolecules in which macrocycles (beads) encircle a dumbbell-like linear molecules (threads).[3] A variety of organic macrocycles have been used as the bead component for the preparation of the rotaxanes.[4–7] Instead of these organic macrocycles, exploitation of transition-metal-bridged metallomacrocycles[8] would be interesting because transition metals are generally more sensitive and responsive on the electrochemical and light stimuli relative to organic molecules.[9] Therefore, incorporation of a transition metal into the rotaxane[10, 11] may give an opportunity to develop more versatile rotaxane-based machines.

We reported for the first time the metallomacrocycle-based rotaxane **2-Os**, self-assembled from the osmate ester-bridged metallomacrocycle **1-Os** and the thread **3**.[12] However, the metallomacrocycle-based rotaxane **2-Os** is kinetically so labile that it behaves like the pseudorotaxane rather than the conventional covalent rotaxane. The kinetic stability[13, 14] of the metallomacrocycle-based rotaxane[15] is directly related to the strength of the coordination bond in the metallomacrocycle, and can be tuned by varying the combination of transition metal and ligand. It would be an ideal case that the coordination bond is reversible at higher temperatures for the self-assembly of the rotaxane, but irreversible around room temperature for convenient isolation and handling under ordinary laboratory conditions.[16] With this in mind, we report here on the preparation of three new metallomacrocycle-based rotaxanes (**2-Pd**, **2-Pt**, and **2-Re**), which contain the most widely used metallic units for the self-assembly of supramolecular entities (Scheme 1).[8, 17] The kinetic stabilities of these rotaxanes were quantitatively measured and compared with one another by $^1$H NMR spectroscopic techniques, including 2D-EXSY experiments. In particular, the metallomacrocycle-based rotaxane **2-Re** was found to be kinetically the most stable one; we were able to isolate it in pure form by silica gel column chromatography.

[a] Prof. Dr. K.-S. Jeong, S.-Y. Chang, H.-Y. Jang
Department of Chemistry, Yonsei University
Seoul 120-749 (South Korea)
Fax: (+82) 2-364-7050
E-mail: ksjeong@yonsei.ac.kr

Supporting information for this article is available on the WWW under http://www.chemeurj.org or from the author.

  0947-6539/03/0907-1535 $ 20.00+.50/0 

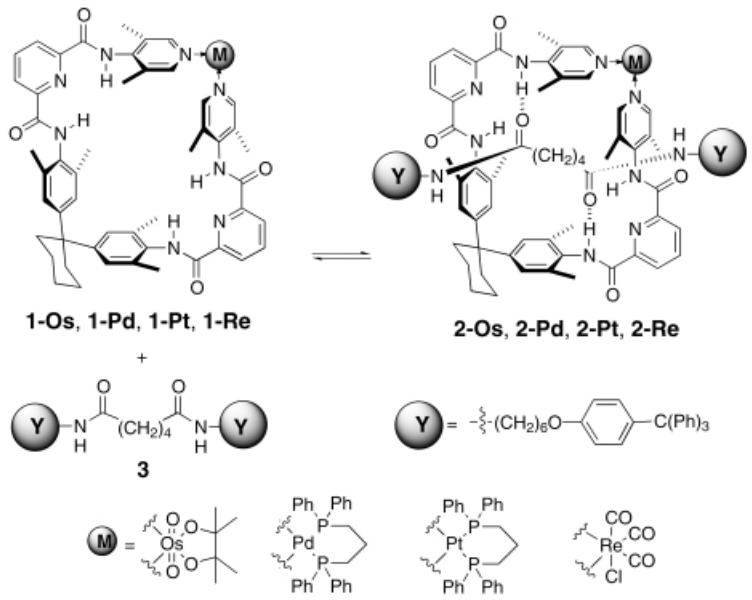


Scheme 1. Self-assembly of rotaxanes, **2-Os**, **2-Pd**, **2-Pt**, and **2-Re**.

## Results and Discussion

**Syntheses and characterization of metallomacrocycles 1-Os, 1-Pd, 1-Pt, and 1-Re**: The metallomacrocycle **1-Os** and its precursor bispyridyl ligand were prepared as described previously.[18] The metallomacrocycles **1-Pd** and **1-Pt** were prepared in 93–94% yield at room temperature by simply mixing the ligand and $[M(dppp)(CF_3SO_3)_2]$ (M = Pd or Pt, dppp = 1,3-bis(diphenylphosphino)propane) at a molar ratio of 1:1 in dichloromethane. The metallomacrocycle **1-Re** was prepared in 93% yield by heating a 1:1 mixture of the ligand and $[Re(CO)_5Cl]$ in 1,1,2,2-tetrachloroethane at 100 °C for 2 hours. These metallomacrocycles were all sufficiently soluble in organic solvents including chloroform, dichloromethane, and acetonitrile. Elemental analyses of the products were consistent with the molecular formula of the metallomacrocycles **1-Pd**, **1-Pt**, and **1-Re**. In the $^1$H NMR spectra, the aryl signals of the lutidyl rings were shifted downfield from those of the free ligand ($\Delta\delta = 0.35$, 0.30, and 0.22 ppm for **1-Pd**, **1-Pt**, and **1-Re**, respectively) as expected on the coordination of the ring nitrogen to the metal center. The FAB-MS analyses also supported the formation of mononuclear metallomacrocycles. For example, the mass spectrum of **1-Pd** showed the molecular ion $[M^+]$ at $m/z = 1646$ (1.3%), along with fragments of $[M^+ - CF_3SO_3]$ and $[M^+ - 2CF_3SO_3]$ at 1495 (33%) and 1345 (9%), respectively. Another cationic metallomacrocycle of **1-Pt** gave a nearly identical pattern of the mass spectrum, while relative intensities for the fragments of $[M^+ - CF_3SO_3]$ ($m/z = 1585$, 71%) and $[M^+ - 2CF_3SO_3]$ ($m/z = 1435$, 12%) were larger relative to those of **1-Pd**. A neutral metallomacrocycle **1-Re** also showed the molecular ion $[M^+]$ ($m/z = 1134$, 9%) and $[M^+ - Cl]$ (m/z = 1099, 25%) in the FAB mass spectrum. Moreover, in all cases the observed isotopic distribution patterns of the molecular ions and fragments were consistent with the calculated ones based on the metallomacrocycles **1-Pd**, **1-Pt**, and **1-Re** (see Supporting Information).

**Syntheses and characterization of [2]rotaxanes 2-Pd, 2-Pt, and 2-Re**: For the self-assembly of the metallomacrocycle-based rotaxanes in this study, the driving force is hydrogen-bonding interactions between the bead and thread components. Therefore, a dumbbell-shaped molecule **3** was chosen as the thread because 1) the adipamide unit strongly binds to the cavity of the bead[18] and 2) the tritylphenyl end group is large enough to prevent the bead slipping off the thread.[12]

When the thread **3** was mixed with either **1-Pd** or **1-Pt** at room temperature in $CDCl_3$, two different sets of $^1$H NMR signals appeared; one for free components and the other for the rotaxane complex (Figure 1). This suggests that the exchange rate between the rotaxane complex and its free components is slow on the NMR timescale. The formation of the rotaxanes **2-Pd** and **2-Pt** was evident in the $^1$H NMR spectra. First, two NH signals of the bead were downfield shifted ($\Delta\delta = 1.3$–1.5 ppm) as the result of hydrogen-bond formation. Second, signals of methylene ($-CH_2-$) between two carbonyls of the adipamide unit in the thread were far upfield shifted from 2.26 and 1.68 ppm to 0.31 and −0.20 ppm, respectively. Interestingly, the magnitudes of the chemical shift changes were

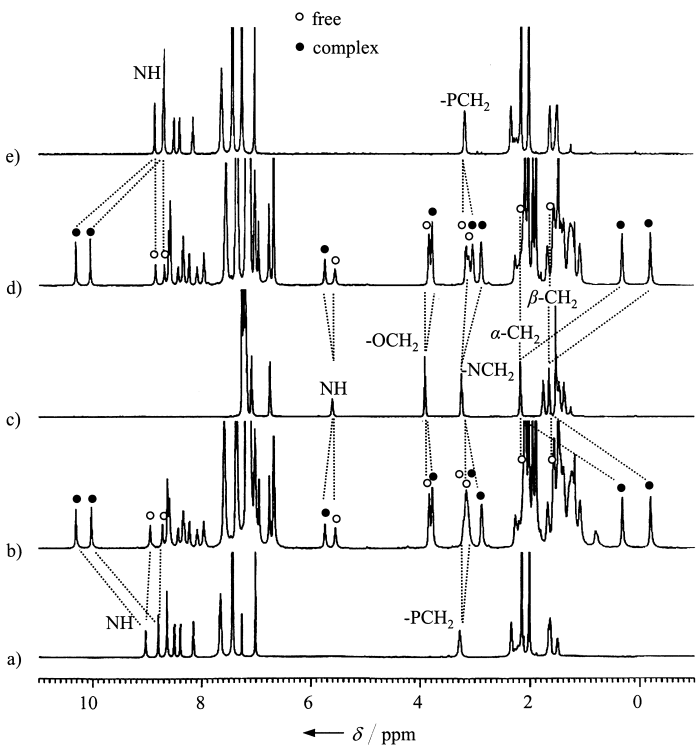


Figure 1. $^1$H NMR (500 MHz) spectra in $CDCl_3$ at 25 °C of a) **1-Pt**, b) **1-Pt** (2 mM) + **3** (2 mM), c) **3**, d) **1-Pd** (2 mM) + **3** (2 mM), and e) **1-Pd**.



0947-6539/03/0907-1536 $ 20.00+.50/0 *Chem. Eur. J.* **2003**, *9*, No. 7

identical to each other on the formation of **2-Pd** and **2-Pt**. These large upfield shifts are a strong evidence for the insertion of the adipamide unit of the thread inside the cavity surrounded by aryl surfaces of the bead. Additional evidence for the self-assembly of the rotaxanes **2-Pd** and **2-Pt** was obtained from the ESI-MS studies of a 1:1 mixture of **3** and **1-Pd** (or **1-Pt**) in $CH_2Cl_2$, showing characteristic peaks that correspond to $[M^+ - CF_3SO_3]$ and $[M^{2+} - 2CF_3SO_3]$ ($M$ = **2-Pd** or **2-Pt**) (see Supporting Information).

In contrast to **2-Pd** and **2-Pt**, the rotaxane **2-Re** could not be self-assembled at room temperature in solution. That is, when two components **1-Re** and **3** were mixed in $Cl_2CDCDCl_2$, no signals other than those of the two reactants were observed for a week at room temperature in the $^1$H NMR spectrum. However, when the temperature was raised to $>60\,^\circ$C, new signals corresponding to **2-Re** slowly appeared in the $^1$H NMR spectrum, and the equilibrium was established in a few hours in $Cl_2CDCDCl_2$. The rotaxane **2-Re** was, therefore, prepared by heating at 70 °C either a 1:1 mixture of **1-Re** and **3** or directly a 1:1:1 mixture of $[Re(CO)_5Cl]$, bispyridyl ligand, and thread **3** in 1,1,2,2-tetrachloroethane. The rotaxane **2-Re** can be isolated in pure form by silica gel chromatography. Elemental analysis, FAB-MS, $^1$H NMR and other spectroscopic data of the isolated product were consistent with the structure of **2-Re** (see Experimental Section and Supporting Information).

**Binding affinities between metallomacrocycles and threads**: Metallomacrocycles **1-Os**, **1-Pd**, **1-Pt**, and **1-Re** are all derived from the same ligand, and thus their overall shapes and sizes are nearly identical to each other. One difference is that **1-Os** and **1-Re** are neutral and **1-Pd** and **1-Pt** are cationic. As mentioned earlier, when **1-Os**, **1-Pd**, and **1-Pt** were mixed with the thread **3** at room temperature, the two components rapidly self-assembled into and established the equilibrium with the corresponding rotaxanes **2-Os**, **2-Pd**, and **2-Pt**. Free components and rotaxanes gave separate $^1$H NMR signals in $CDCl_3$, and binding constants were therefore determined by $^1$H NMR integration method. The binding constants ($K_a \pm 20\,\%$) of metallomacrocycles **1-Pd** and **1-Pt** with the thread **3** were determined to be 1800 and 1500 $M^{-1}$ in $CDCl_3$, respectively, each of which is an average value of four measurements by using 1.0 to 5.0 mM $CDCl_3$ solutions of two components at $24 \pm 1\,^\circ$C (see Supporting Information). For comparison, the binding constant of **1-Os** with **3** was previously reported to be 560 $M^{-1}$ under the same conditions.[12a]

The binding affinity between the metallomacrocycle **1-Re** and the thread **3** cannot be determined at room temperature by either $^1$H NMR integration or titration methods owing to the lack of the equilibrium. Therefore, the binding ability of **1-Re** was indirectly compared with that of **1-Os** by using the thread **6**, which contains smaller phenoxy groups at the ends to form the pseudorotaxane **4** (Scheme 2, later); consequently **1-Re** can be reversibly slipped in and out at room temperature. The $^1$H NMR titration in $CDCl_3$ at $24 \pm 1\,^\circ$C gave the association constant of 1090 $M^{-1}$ between **1-Re** and **6**, which is similar to that of 900 $M^{-1}$ between **1-Os** and **6**.[12a] In conclusion, the binding affinities of two cationic metallomacrocycles **1-Pd** and **1-Pt** are a slightly higher than those of two neutral metallomacrocycles **1-Os** and **1-Re**, but differences in the thermodynamic stabilities of four metallomacrocycle-based rotaxanes are small ($\Delta\Delta G^\circ < 0.7$ kcal mol$^{-1}$).

**Kinetic stabilities of [2]rotaxanes 2-Os, 2-Pd, and 2-Pt**: Due to the presence of weak coordination bonds, the kinetic stability of metallomacrocycle-based rotaxanes is generally much lower than that of the corresponding covalent analogues. The rotaxanes **2-Os**, **2-Pd**, and **2-Pt** can be reversibly converted into their components at room temperature. The rates of interconversions between the rotaxane complexes, **2-Os**, **2-Pd**, and **2-Pt**, and their components are slow on the NMR timescale at room temperature, and, consequently, the rate constants can be determined by two-dimensional exchange spectroscopy (2D-EXSY) experiments.[12, 19] The rate constants were deduced from the diagonal and cross peaks for the NH signals of the metallomacrocycle. The rate constant $k$ for the interconversion between **2-Os** and its components was previously determined to be $24(\pm 4)$ s$^{-1}$, corresponding to an activation energy ($\Delta G^\ddagger$) of 15.5 kcal mol$^{-1}$ at 23 °C.[12a] Similarly, a series of the 2D-EXSY experiments with **2-Pd** and **2-Pt** gave the rate constants of $11.0(\pm 0.3)$ s$^{-1}$ and $6.2(\pm 0.1)$ s$^{-1}$ at 25 °C, respectively. These values correspond to activation free energies ($\Delta G^\ddagger$) of 16.0 kcal mol$^{-1}$ and 16.4 kcal mol$^{-1}$. The kinetic stabilities are therefore in the order of **2-Os** < **2-Pd** < **2-Pt**, but differences ($\Delta\Delta G^\ddagger$) are within 1 kcal mol$^{-1}$. Consequently, the metallomacrocycle-based rotaxanes **2-Os**, **2-Pd**, and **2-Pt** are all kinetically labile and exist only in equilibrium mixtures with their components at room temperature.

**Kinetic stability of [2]rotaxane 2-Re**: The rotaxane **2-Re** does not disassemble into its components at room temperature. However, at elevated temperatures it slowly disassembles into its components **1-Re** and **3** until the equilibrium is established. This process can be quantitatively monitored by $^1$H NMR spectroscopy (Figure 2a), and the rate constant can be estimated from Equations (1) – (4).[20]

$$\mathrm{R} \underset{k_{on}}{\overset{k_{off}}{\rightleftharpoons}} \mathrm{M} + \mathrm{T} \tag{1}$$

$$A \ln B = k_{off} t \tag{2}$$

$$A = \left( \frac{[\mathrm{R}]_0 - [\mathrm{R}]_e}{[\mathrm{R}]_0 + [\mathrm{R}]_e} \right) \tag{3}$$

$$B = \left( \frac{[\mathrm{R}]_0^2 - [\mathrm{R}]_e[\mathrm{R}]}{[\mathrm{R}]_0([\mathrm{R}] - [\mathrm{R}]_e)} \right) \tag{4}$$

in which R, M, and T refer to rotaxane, metallomacrocycle, and thread, respectively, $[R]_0$, $[R]_e$, and $[R]$ are initial concentration of the rotaxane, concentration at equilibrium, and concentration at time $t$, respectively, and $k_{off}$ and $k_{on}$ are rate constants of the disassembly and of the assembly of the rotaxane, respectively. Here, $[R]$ and $[R]_e$ can be experimentally measured by the $^1$H NMR integration, while $[R]_0$ is known.

The experiments were performed by using a solution of **2-Re** in $Cl_2CDCDCl_2$ (5 mM) at three different temperatures (60, 70, and 80 °C). In each experiment, a well-correlated linear relationship was observed from the plot of $A \ln B$

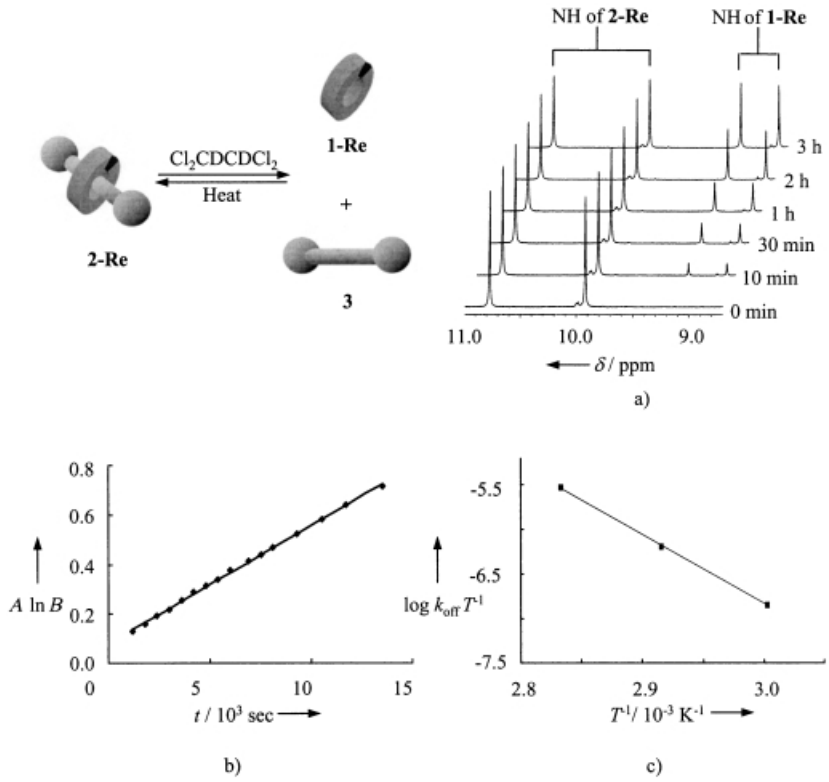


Figure 2. a) Partial $^1$H NMR (500 MHz) spectra showing the disassembly of the rotaxane **2-Re** (5 mM) at 60 °C in $Cl_2CDCDCl_2$ at $t = 0$ min, 10 min, 30 min, 1 h, 2 h, and 3 h. b) Plot of $A \ln B$ against $t$, whereby the slope corresponds to the rate constant $k_{off}$ of the disassembly of **2-Re** at 60 °C. c) Eyring plot for the disassembly of **2-Re** into its components.

against time ($t$), whereby the slope corresponds to the rate constant $k_{off}$ for the disassembly of the rotaxane **2-Re** (Figure 2b and also see Supporting Information). From the constant $k_{off}$ and the equilibrium constant $K$ at the given temperature, the formation rate constant $k_{on}$ of the **2-Re** can be also calculated. All of these values along with the corresponding free energies are summarized in Table 1. From the Eyring equation, the plot of $\log(k_{off} T^{-1})$ against $T^{-1}$[21] gave an activation enthalpy $\Delta H^{\ddagger}$ of 35 kcal mol$^{-1}$ and an activation entropy $\Delta S^{\ddagger}$ of 27 eu for the disassembly of **2-Re** (Figure 2c). Extrapolation of the plot gave the dissociation rate constant $k_{off}$ of $8.0 \times 10^{-8}$ s$^{-1}$ at 25 °C, corresponding to the activation free energy $\Delta G^{\ddagger}_{off}$ of 27.1 kcal mol$^{-1}$. This magnitude is approximately 11 kcal mol$^{-1}$ higher than those of **2-Pd** and **2-Pt**. It is also worthwhile mentioning that the rotaxane **2-Re** remains intact in the solid state around room temperature (20–30 °C) for about six months, as we examined so far.

To reveal the mechanism for the disassembly of **2-Re**, the activation energies for two more rhenium-based (pseudo)-rotaxanes **4** and **5**, which contain different sizes of end groups, were examined. First, in the case of smaller phenoxy end group, the assembly and disassembly of the complex **4** was fast on the NMR timescale at room temperature. The activation free energy of this process was calculated to be $12.1 \pm 0.1$ kcal mol$^{-1}$, based on the coalescence temperatures of $OCH_2$ (−22 °C) and $NCH_2$ (−20 °C) signals in $CDCl_3$.[21a] The complex **4** can be formed reversibly by slipping the metallomacrocycle **1-Re** on and off the thread over the small phenoxy end group without dissociation of the Re–N coordination bond (Scheme 2). Second, in the rotaxane **5**, which has a much larger 4-tris(4-*tert*-butylphenyl)-methylphenoxy end group, the activation free energy for the disassembly process was measured by the identical method used for **2-Re**, and calculated to be ~26.2 kcal mol$^{-1}$ at 60 °C. The kinetic stabilities of two rhenium-based rotaxanes **2-Re** and **5** are identical to each other, despite a large difference in the size of the stoppers. These results strongly support that the disassembly of both **2-Re** and **5** occurs through a clipping process, that is, the dissociation of the Re–N coordination bond, followed by disassembly of the intermediate complex and reassociation of the coordination bond (Scheme 2).

Table 1. Rate constants ($k_{off}$, $k_{on}$), activation free energies ($\Delta G^{\ddagger}_{off}$, $\Delta G^{\ddagger}_{on}$), and equilibrium constants ($K$) for the disassembly and assembly of **2-Re** at each temperature.

| Entry | $T$ [°C] | $k_{off}$ [s$^{-1}$] | $\Delta G^{\ddagger}_{off}$ [kcal mol$^{-1}$] | $k_{on}$ [s$^{-1}$] | $\Delta G^{\ddagger}_{on}$ [kcal mol$^{-1}$] | $K$ [M$^{-1}$] |
|---|---|---|---|---|---|---|
| 1 | 60 | $4.78 \times 10^{-5}$ | 26.2 | $3.51 \times 10^{-3}$ | 23.3 | 73 |
| 2 | 70 | $2.23 \times 10^{-4}$ | 25.9 | $1.24 \times 10^{-2}$ | 23.2 | 56 |
| 3 | 80 | $1.04 \times 10^{-3}$ | 25.6 | $3.70 \times 10^{-2}$ | 23.1 | 36 |

## Conclusion

The reversible self-assembly is of a great advantage to the supramolecular synthesis, but unfortunately results in a decrease in the kinetic stability. A fine balance of these opposite properties is required for the development of more easily accessible but robust supramolecular machines. The rhenium-based rotaxane described here is found to be one such an entity. In addition, the system of the metallomacrocycle-based rotaxane has been demonstrated to be a powerful tool to obtain the quantitative information on the strength of the coordination bond.

## Experimental Section

**General methods**. All reagents were, unless otherwise noted, used as received. Dichloromethane was distilled under nitrogen from calcium hydride ($CaH_2$), and diethyl ether from Na/benzophenone. Melting points were determined by using a Mel-Temp II capillary melting point apparatus and were uncorrected. Infrared spectra were obtained on a Nicolet impact 410 FT-IR spectrometer. All NMR spectra were recorded on a DRX-500



0947-6539/03/0907-1538 $ 20.00+.50/0 *Chem. Eur. J.* **2003**, *9*, No. 7

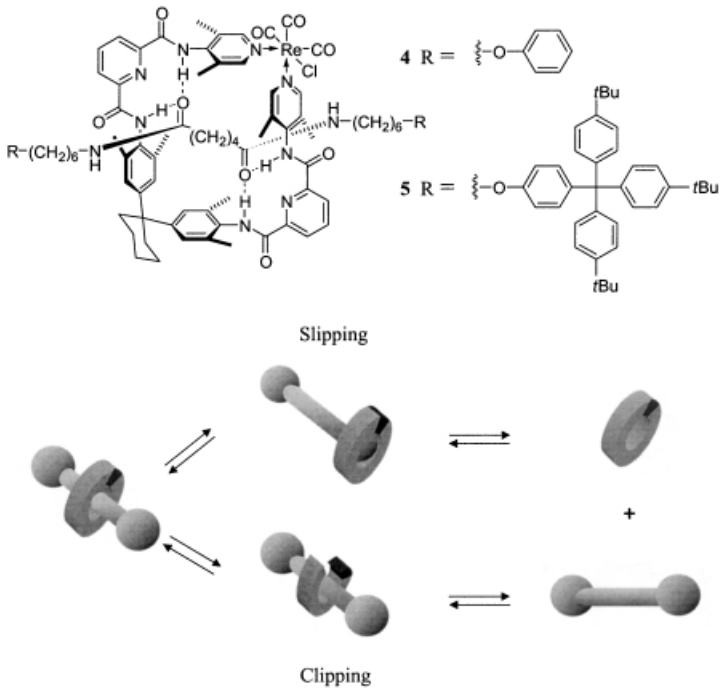


Scheme 2. Structures of **4** and **5**, and schematic representation of two possible pathways: slipping and clipping.

spectrometer, and chemical shifts were reported in ppm downfield relative to the residual protonated solvent peaks ($CHCl_3$: $\delta = 7.26$ ppm for $^1H$ NMR spectra, $\delta = 77$ ppm for $^{13}C$ NMR spectra). FAB-MS spectra were obtained with a JMS-HS 110/110A mass spectrometer (JEOL, Japan), and nitrobenzyl alcohol was used as a matrix in $CHCl_3$ as solvent. ESI-MS spectra were obtained with a QUATTRO LC triple quadrupole tandem mass spectrometer (Micromass, UK).

**Metallomacrocycle 1-Pd**: A solution of precursor bispyridyl ligand[18a] (33 mg, 0.040 mmol) and [Pd(dppp)$OTf_2$][22] (33 mg, 0.040 mmol, 1 equiv) in $CH_2Cl_2$ (5 mL) was stirred at room temperature for 3 h under argon. Diethyl ether was added to the solution to give **1-Pd** as a white precipitate. The precipitate was washed with diethyl ether and dried under reduced pressure to give a white solid (62 mg, 94%). M.p. >250 °C; $^1H$ NMR (500 MHz, $CDCl_3$, 25 °C): $\delta = 8.89$ (s, 2H; NH), 8.73 (s, 2H; NH), 8.68 (s, 4H; lutidyl H), 8.51 (d, $^3J(H,H) = 7.7$ Hz, 2H; pyridyl H), 8.41 (d, $^3J(H,H) = 7.7$ Hz, 2H; pyridyl H), 8.16 (t, $^3J(H,H) = 7.7$ Hz, 2H; pyridyl H), 7.63 (brs, 8H; phenyl H), 7.43 (brs, 12H; phenyl H), 7.02 (s, 4H; anilinyl H), 3.18 (brs, 4H; $PCH_2$), 2.34–2.28 (m, 6H; cyclohexyl H, $PCH_2CH_2$), 2.16 (s, 12H; $ArCH_3$), 2.02 (s, 12H; $ArCH_3$), 1.64 ppm (brs, 6H; cyclohexyl H); $^{13}C$ NMR (125 MHz, $CDCl_3$, 25 °C): $\delta = 160.8$, 160.2, 149.2, 148.2, 147.3, 144.5, 139.8, 134.8, 133.3, 132.7, 130.1, 129.6, 126.2, 125.3, 44.9, 35.3, 31.6, 29.7, 26.3, 22.8, 22.6, 21.6, 18.9, 17.6, 15.5, 14.1 ppm; IR(KBr): $\tilde{\nu} = 3450$ (NH), 1679 (C=O), 1258 (OTf), 1165 (OTf), 1034 $cm^{-1}$ (OTf); FAB-MS (*m*NBA matrix, based on $^{106}Pd$): *m*/*z* (%): 1646.1 (1.3) [$M^+$], 1495.2 (33) [$M^+ - OTf$], 1345.2 (8.5) [$M^+ - 2OTf$]; elemental analysis calcd for $C_{79}H_{78}F_6N_8O_{10}P_2PdS_2$ (1646.00): C 57.65, H 4.78, N 6.81, S 3.90; found: C 57.70, H 4.98, N 6.89, S 3.74.

**Metallomacrocycle 1-Pt**: Metallomacrocycle **1-Pt** was synthesized from the bispyridyl ligand and [Pt(dppp)$OTf_2$][22] by the same method used for the synthesis of **1-Pd** except for the reaction time of 11 h. A white solid was isolated (93%). M.p. >250 °C; $^1H$ NMR (500 MHz, $CDCl_3$, 25 °C): $\delta = 9.06$ (s, 2H; NH), 8.82 (s, 2H; NH), 8.63 (s, 4H; lutidyl H), 8.51 (d, $^3J(H,H) =$ 7.7 Hz, 2H; pyridyl H), 8.39 (d, $^3J(H,H) = 7.7$ Hz, 2H; pyridyl H), 8.16 (t, $^3J(H,H) = 7.8$ Hz, 2H; pyridyl H), 7.65 (brs, 8H; phenyl H), 7.43 (brs, 12H; phenyl H), 7.01 (s, 4H; anilinyl H), 3.27 (brs, 4H; $PCH_2$), 2.33–2.27 (m, 6H; cyclohexyl H, $PCH_2CH_2$), 2.15 (s, 12H; $ArCH_3$), 2.01 (s, 12H; $ArCH_3$), 1.65 ppm (brs, 6H; cyclohexyl H); $^{13}C$ NMR (125 MHz, $CDCl_3$, 25 °C): $\delta =$ 160.8, 160.1, 149.2, 149.0, 148.2, 147.1, 145.1, 139.8, 134.8, 134.0, 132.8, 130.0, 129.5, 126.2, 125.4, 124.3, 44.9, 35.2, 26.4, 22.8, 21.7, 21.5, 21.4, 18.9, 17.6, 15.6 ppm; IR(KBr): $\tilde{\nu} = 3489$ (NH), 1683 (C=O) 1258 (OTf), 1165 (OTf), 1034 $cm^{-1}$ (OTf); FAB-MS (*m*NBA matrix, based on $^{195}Pt$): *m*/*z* (%): 1735.2 (1.1) [$M^+$], 1585.2 (71) [$M^+ -$ OTf], 1435.2 (12) [$M^+ - 2OTf$]; elemental analysis calcd for $C_{79}H_{78}F_6N_8O_{10}P_2PtS_2 \cdot 3H_2O$ (1752.67): C 53.05, H 4.73, N 6.26, S 3.59; found: C 53.33, H 4.83, N 6.15, S 3.56.

**Metallomacrocycle 1-Re**: A solution of the bispyridyl ligand (0.25 g, 0.30 mmol) and [$Re(CO)_5Cl$] (0.11 g, 0.30 mmol, 1 equiv) in 1,1,2,2-tetrachloroethane (15 mL) was stirred at 100 °C for 2 h under argon; hexane was then added to the solution to give **1-Re** as a white precipitate. The precipitate was washed with hexane and dried under reduced pressure to give a white solid (0.32 g, 93%). M.p. >250 °C; $^1H$ NMR (500 MHz, $CDCl_3$, 25 °C): $\delta = 9.26$ (s, 2H; NH), 8.83 (s, 2H; NH), 8.59–8.53 (m, 8H; lutiyl H, pyridyl H), 8.24 (t, $^3J(H,H) = 7.7$ Hz, 2H; pyriyl H), 7.05 (s, 4H; anilinyl H), 2.32 (brs, 4H; cyclohexyl H), 2.28 (s, 12H; $ArCH_3$), 2.23 (s, 12H; $ArCH_3$), 1.66 ppm (brs, 6H; cyclohexyl H); $^{13}C$ NMR (125 MHz, $CDCl_3$, 25 °C): $\delta = 195.0$, 192.7, 160.7, 160.0, 153.0, 148.9, 148.8, 147.3, 143.8, 140.2, 134.8, 131.1, 130.2, 126.8, 126.4, 125.9, 45.1, 35.9, 26.2, 22.8, 19.1, 16.1 ppm; IR(KBr): $\tilde{\nu} = 3463$ (NH), 2024 (Re(C=O)), 1921 (Re(C=O)), 1885 (Re(C=O)), 1693 $cm^{-1}$ (amide C=O); FAB-MS (*m*NBA matrix, based on $^{187}Re$): *m*/*z* (%): 1134.3 (9.3) [$M^+$], 1099.4 (25) [$M^+ -$Cl]; elemental analysis calcd for $C_{53}H_{52}ClN_8O_7Re$ (1134.69): C 56.10, H 4.62, N 9.88; found: C 56.17, H 4.88, N 9.78.

**Rotaxane 2-Re**: A solution of **1-Re** (116 mg, 0.102 mmol) and thread **3**[12a] (100 mg, 0.102 mmol, 1 equiv) in 1,1,2,2-tetrachloroethane (0.5 mL) was stirred at 70 °C for 7 h. Rotaxane **2-Re** was obtained as a white solid (134 mg, 62%) after flash column chromatography (EtOAc/$CH_2Cl_2$ 1:8). The use of precursor bispyridyl ligand and [$Re(CO)_5Cl$] instead of **1-Re** with thread **3** also gave the same rotaxane **2-Re** (53%). M.p. 176 °C (decomp); $^1H$ NMR (500 MHz, $CDCl_3$, 25 °C): $\delta = 10.90$ (s, 2H; NH), 10.16 (s, 2H; NH), 8.50 (s, 4H; lutidyl H), 8.46 (d, $^3J(H,H) = 7.5$ Hz, 2H; pyridyl H), 8.39 (d, $^3J(H,H) = 7.5$ Hz, 2H; pyridyl H), 8.05 (t, $^3J(H,H) = 7.6$ Hz, 2H; pyridyl H), 7.24–7.18 (m, 30H; phenyl H), 7.11 (d, $^3J(H,H) = 7.9$ Hz, 4H; phenyl H), 6.97 (s, 4H; anilinyl H), 6.73 (m, 4H; phenyl H), 5.48 (s, 1H; NH), 5.29 (s, 1H; NH), 3.82 (t, $^3J(H,H) = 8.3$ Hz, 4H; $OCH_2$), 2.96 (t, $^3J(H,H) = 6.8$ Hz, 4H; $NCH_2$), 2.27 (brs, 4H; cyclohexyl H), 2.23 (s, 12H; $ArCH_3$), 2.18 (s, 12H; $ArCH_3$), 1.59 (brs, 6H; cyclohexyl H), 1.50 (brs, 4H; $CH_2$), 1.36 (brs, 4H; $CH_2$), 1.26 (brs, 4H; $CH_2$), 1.16 (brs, 4H; $CH_2$), 0.90 (brs, 2H; $(C=O)CH_2$), 0.83 (brs, 2H; $(C=O)CH_2$), 0.21 ppm (brs, 4H; $(C=O)\ CH_2CH_2$); $^{13}C$ NMR (125 MHz, $CDCl_3$, 25 °C): $\delta = 195.0$, 192.8, 173.1, 173.0, 162.0, 161.6, 156.8, 156.7, 152.6, 149.2, 148.4, 147.8, 147.0, 145.5, 139.5, 139.1, 139.0, 135.3, 132.9, 132.2, 131.4, 131.1, 127.4, 126.5, 125.8, 125.7, 125.2, 113.2, 113.1, 67.3, 67.2, 64.3, 44.8, 40.0, 39.9, 36.2, 36.1, 34.3, 34.1, 29.4, 29.3, 29.1, 26.7, 26.2, 25.8, 25.7, 22.9, 22.7, 18.9, 15.9 ppm; IR(KBr): $\tilde{\nu} = 3257$ (NH), 2026 (Re(C=O)), 1922 (Re(C=O)), 1887 (Re(C=O)), 1693 (amide C=O), 1646 $cm^{-1}$ (amide C=O); FAB-MS (*m*NBA matrix, based on $^{187}Re$): *m*/*z* (%): 2116.0 (58) [$M^+$+H], 2080.0 (22) [$M^+ -$ Cl]; elemental analysis calcd for $C_{121}H_{124}ClN_{10}O_{11}Re$ (2116.00): C 68.68, H 5.91, N 6.62; found C 68.82, H 5.88, N 6.45.

**Rotaxane 5**: The rotaxane **5** was prepared from **1-Re** and the corresponding thread[12b] by following the method used for the preparation of **2-Re**, and was purified with flash column chromatography (EtOAc/$CH_2Cl_2$ 1:10) to give a white solid (39%). M.p. 230 °C (decomp); $^1H$ NMR (500 MHz, $CDCl_3$, 25 °C): $\delta = 10.90$ (s, 2H; NH), 10.14 (s, 2H; NH), 8.50 (s, 4H; lutidyl H), 8.45 (d, $^3J(H,H) = 7.3$ Hz, 2H; pyridyl H), 8.38 (d, $^3J(H,H) = 7.3$ Hz, 2H; pyridyl H), 8.03 (t, $^3J(H,H) = 7.2$ Hz, 2H; pyridyl H), 7.23–7.08 (m, 28H; phenyl H), 6.97 (s, 4H; anilinyl H), 6.72 (brs, 4H; phenyl H), 5.38 (s, 1H; NH), 5.24 (s, 1H; NH), 3.80 (brs, 4H; $OCH_2$), 2.97 (brs, 4H; $NCH_2$), 2.23 (brs, 16H; cyclohexyl H, $ArCH_3$), 2.18 (s, 12H, $ArCH_3$), 1.60–1.16 (m, 70H; $CH_2$, *t*-Bu), 0.89 (brs, 2H; $(C=O)\ CH_2$), 0.83 (brs, 2H; $(C=O)CH_2$),

0.21 ppm (br s, 4H; (C=O)$CH_2CH_2$); $^{13}$C NMR (125 MHz, $CDCl_3$, 25 °C): $\delta$ = 194.9, 192.7, 173.0, 172.9, 162.0, 161.5, 156.7, 156.6, 152.6, 149.1, 148.3, 148.2, 147.7, 145.5, 144.1, 139.6, 139.5, 135.2, 132.9, 132.2, 131.4, 130.6, 126.5, 125.7, 125.2, 124.0, 112.8, 112.7, 67.2, 67.1, 63.0, 44.8, 40.0, 39.9, 36.2, 36.0, 34.3, 34.0, 31.3, 29.7, 29.4, 29.3, 29.2, 26.8, 26.2, 25.8, 25.7, 22.7, 18.9, 15.9 ppm; IR(KBr): $\tilde{\nu}$ = 3269 (NH), 2027 (Re(C=O)), 1926 (Re(C=O)), 1891 (Re(C=O)), 1696 (amide C=O), 1646 cm$^{-1}$ (amide C=O); FAB-MS (*m*NBA matrix, based on $^{187}$Re): *m*/*z* (%): 2452.7 (1.1) [$M^+$+H], 2416.7 (7.5) [$M^+$ − Cl]; elemental analysis calcd for $C_{145}H_{172}ClN_{10}O_{11}Re$ (2452.64): C 71.01, H 7.07, N 5.71; found: C 71.29, H 7.31, N 5.62.

**Determination of binding constants**

**a) $^1$H NMR titration method**:[18, 23] Chloroform was stored over 4 Å molecular sieves and treated with $K_2CO_3$ prior to use. A 2 mM solution of host (**1-Re**) and 10 mM solution of the guest (**6**) in $CDCl_3$ (2 mL) were separately prepared. A 500 μL portion of the host solution was transferred to a NMR tube, and an initial NMR spectrum was taken to determine the initial chemical shift ($\delta_{free}$) of the free host. Aliquots of the guest solution (10 μL initially, then 20–30 μL, and finally 50–100 μL) were added to the host solution. The spectrum was recorded after each addition and overall 11 data points were obtained. The association constants ($K_a$) were determined by using the nonlinear least-squares fitting of the titration curve plot $\Delta\delta$ of the host NH signals against the molar equivalent of the guest. All of the titration curves were well fitted to the expression of a 1:1 binding isotherm shown below [Eqs. (5)–(8)].

$$H + G \rightleftharpoons HG \tag{5}$$

$$K_a = \frac{[HG]}{[H][G]} \tag{6}$$

$$\Delta\delta = \frac{\Delta\delta_{max}}{2[H]}\left[K_a^{-1} + [H]_t + [G]_t - \sqrt{(K_a^{-1} + [H]_t + [G]_t)^2 - 4[H]_t[G]_t}\right] \tag{7}$$

$$\chi^2 = \Sigma(\Delta\delta_{calcd} - \Delta\delta_{obsvd})^2 \tag{8}$$

Here, $[H]_t$ and $[G]_t$ are the total concentrations of host and guest, $K_a$ is the association constant, $\Delta\delta_{calcd}$ and $\Delta\delta_{obsvd}$ are the calculated and observed chemical shift change at the each titration point, and $\delta\delta_{max}$ is the maximum chemical shift change when complexation is completed. Minimizing the sum of the squared deviations $\chi^2$ affords the association constant ($K_a$), along with $\Delta\delta_{max\ (calcd)}$.

**b) $^1$H NMR integration method**: Four solutions containing a 1:1 molar mixture of metallomacrocycle **1-Pd** (or **1-Pt**) and thread **3** were separately prepared. The concentrations of both components were 1.0, 2.0, 3.0, and 5.0 mM, respectively. The $^1$H NMR spectrum of each solution was recorded at 24 ± 1 °C. The concentrations of $[H]_{free}$, $[G]_{free}$, and [HG] were deduced from the integrations of well-separated signals: NHs of **1-Pd** or **1-Pt** and NH of **3**.

**2D-EXSY experiments**:[12, 19] The 2D-EXSY spectra were recorded at 298 K on an 500 MHz Bruker spectrometer. The mixing time was 100 ms, and each of 128 $F_1$ increments was the accumulation of 32 scans. Prior to Fourier transformation, the FIDs were multiplied by a square sine bell 90° shifted in the $F_1$ and 60° shifted in the $F_2$ domains. The data file was zero-filled, affording a spectrum of 2K × 256K real data points. The rate constants ($k$) were calculated employing the Equations (9)–(13) below, in which $\tau_m$ is mixing time, $I_{AB}$ and $I_{BA}$ are cross peak intensities, $I_{AA}$ and $I_{BB}$ are diagonal peak intensities, and $X_A$, $X_B$ are molar fractions of the free component and complex which was determined by $^1$H NMR integration ($R$ = 1.9872 cal K$^{-1}$ mol$^{-1}$; $k_B$ = 3.2995 × 10$^{-24}$ cal K$^{-1}$; $h$ = 1.5836 × 10$^{-34}$ cal s).

$$A \underset{k_{-1}}{\overset{k_1}{\rightleftharpoons}} B \tag{9}$$

$$k = k_1 + k_{-1} \tag{10}$$

$$k = \frac{1}{\tau_m}\ln\frac{r+1}{r-1} \tag{11}$$

$$r = 4X_AX_B\frac{(I_{AA} + I_{BB})}{(I_{AB} + I_{BA})} - (X_A - X_B)2 \tag{12}$$

$$\Delta G^{\ddagger} = -RT\ln\frac{kh}{k_BT} \tag{13}$$

**Determination of the rate constant of 2-Re**: A 5 mM solution of **2-Re** in $Cl_2CDCDCl_2$ was prepared and a 500 μL aliquot was transferred to a 5 mm NMR tube. The spectrum was recorded at appropriate time intervals (5–30 min) at 60, 70, or 80 °C until the ratio of the rotaxane and its components remained constant. Concentrations of the rotaxane at time $t$ were measured from the $^1$H NMR integration of the NH signals of the bead. The rate constant $k_{off}$ was estimated from the slope of the plot of $A \ln B$ [Eq. (2); see the text] against time.

## Acknowledgements

This work was financially supported by the Korea Science and Engineering Foundation (R02-2001-000-00035-0).

[1] For reviews on molecular machines see: a) V. Balzani, A. Credi, F. M. Raymo, J. F. Stoddart, *Angew. Chem.* **2000**, *112*, 3484–3530; *Angew. Chem. Int. Ed.* **2000**, *39*, 3348–3391; b) special issue on molecular machines: *Acc. Chem. Res.* **2001**, *34*, 412–522.

[2] a) J. O. Jeppesen, J. Perkins, J. Becher, J. F. Stoddart, *Angew. Chem.* **2001**, 113, 1256–1261; *Angew. Chem. Int. Ed.* **2001**, *40*, 1216–1221; b) A. M. Brouwer, C. Frochot, F. G. Gatti, D. A. Leigh, L. Mottier, F. Paolucci, S. Roffia, G. W. H. Wurpel, *Science*, **2001**, *291*, 2124–2128; c) G. W. H. Wurpel, A. M. Brouwer, I. H. M. van Stokkum, A. Farran, D. A. Leigh, *J. Am. Chem. Soc.* **2001**, *123*, 11327–11328; d) C. P. Collier, J. O. Jeppesen, Y. Luo, J. Perkins, E. W. Wong, J. R. Heath, J. F. Stoddart, *J. Am. Chem. Soc.* **2001**, *123*, 12632–12641; e) R. Ballardini, V. Balzani, M. Clemente-León, A. Credi, M. T. Gandolfi, E. Ishow, J. Perkins, J. F. Stoddart, H.-R. Tseng, S. Wenger, *J. Am. Chem. Soc.* **2002**, *124*, 12786–12795; f) C. A. Stanier, S. J. Alderman, T. D. W. Claridge, H. L. Anderson, *Angew. Chem.* **2002**, *114*, 1847–1850; *Angew. Chem. Int. Ed.* **2002**, *41*, 1769–1772; g) M. C. Jimenez-Molero, C. Dietrich-Buchecker, J.-P. Sauvage, *Chem. Eur. J.* **2002**, *8*, 1456–1466.

[3] For reviews on pseudorotaxanes and rotaxanes, see: a) R. Jäger, F. Vögtle, *Angew. Chem.* **1997**, *109*, 966–980; *Angew. Chem. Int. Ed. Engl.* **1997**, *36*, 930–944; b) J.-C. Chambron, J.-P. Sauvage, *Chem. Eur. J.* **1998**, *4*, 1362–1366; c) S. A. Nepogodiev, J. F. Stoddart, *Chem. Rev.* **1998**, *98*, 1959–1976; d) C. Seel, F. Vögtle, *Chem. Eur. J.* **2000**, *6*, 21–24; e) T. J. Hubin, D. H. Busch, *Coord. Chem. Rev.* **2000**, *200–202*, 5–52; f) K. Kim, *Chem. Soc. Rev.* **2002**, *31*, 96–107.

[4] a) J. O. Jeppesen, J. Perkins, J. Becher, J. F. Stoddart, *Org. Lett.* **2000**, *2*, 3547–3550; b) A. Arduini, R. Ferdani, A. Pochini, A. Secchi, F. Ugozzoli, *Angew. Chem.* **2000**, *112*, 3595–3598; *Angew. Chem. Int. Ed.* **2000**, *39*, 3453–3456; c) M. J. MacLachlan, A. Rose, T. M. Swager, *J. Am. Chem. Soc.* **2001**, *123*, 9180–9181; d) X. Zhao, X.-K. Jiang, M. Shi, Y.-H. Yu, W. Xia, Z.-T. Li, *J. Org. Chem.* **2001**, *66*, 7035–7043; e) J. M. Mahoney, R. Shukla, R. A. Marshall, A. M. Beatty, J. Zajicek, B. D. Smith, *J. Org. Chem.* **2002**, *67*, 1436–1440; f) J. A. Wisner, P. D. Beer, M. G. B. Drew, M. R. Sambrook, *J. Am. Chem. Soc.* **2002**, *124*, 12469–12476; g) M. Andersson, M. Linke, J.-C. Chambron, J. Davidsson, V. Heitz, L. Hammarström, J.-P. Sauvage, *J. Am. Chem. Soc.* **2002**, *124*, 4347–4362.

[5] For recent examples of lactam macrocycle-based rotaxanes, see: a) C. Reuter, W. Wienand, C. Schmuck, F. Vögtle, *Chem. Eur. J.* **2001**, *7*, 1728–1733; b) F. G. Gatti, D. A. Leigh, S. A. Nepogodiev, A. M. Z. Slawin, S. J. Teat, J. K. Y. Wong, *J. Am. Chem. Soc.* **2001**, *123*, 5983–5989; c) M. Asakawa, G. Brancato, M. Fanti, D. A. Leigh, T. Shimizu, A. M. Z. Slawin, J. K. Y. Wong, F. Zerbetto, S. Zhang, *J. Am. Chem. Soc.* **2002**, *124*, 2939–2950; d) C. A. Schalley, G. Silva, C. F. Nising, P. Linnartz, *Helv. Chim. Acta* **2002**, *85*, 1578–1596.

[6] For recent examples of crown ether macrocycle-based rotaxanes, see: a) S.-H. Chiu, S. J. Rowan, S. J. Cantrill, J. F. Stoddart, A. J. P. White, D. J. Williams, *Chem. Eur. J.* **2002**, *8*, 5170–5183; b) J. Tiburcio, G. J. E. Davidson, S. J. Loeb, *Chem. Commun.* **2002**, 1282–1283; c) Y. Tokunaga, T. Seo, *Chem. Commun.* **2002**, 970–971; d) H. W. Gibson, N. Yamaguchi, L. Hamilton, J. W. Jones, *J. Am. Chem. Soc.* **2002**, *124*, 4653–4665; e) S.-H. Chiu, A. M. Elizarov, P. T. Glink, J. F. Stoddart, *Org. Lett.* **2002**, *4*, 3561–3564; f) Y. Furusho, G. A. Rajkumar, T. Oku, T. Takata, *Tetrahedron* **2002**, *58*, 6609–6613.

  0947-6539/03/0907-1540 $ 20.00+.50/0 

[7] For cyclodextrin-based rotaxanes, see: a) H. Shigekawa, K. Miyake, J. Sumaoka, A. Harada, M Komiyama, *J. Am. Chem. Soc.* **2000**, *122*, 5411–5412; b) T. Fujimoto, Y. Sakata, T. Kaneda, *Chem. Commun.* **2000**, 2143–2144; c) I. Yamaguchi, K. Osakada, T. Yamamoto, *Chem. Commun.* **2000**, 1335–1336; d) H, Onagi, C. J. Easton, S. F. Lincoln, *Org. Lett.* **2001**, *3*, 1041–1044; e) C. A. Stanier, M. J. O'Connell, W. Clegg, H. L. Anderson, *Chem. Commun.* **2001**, 493–494.

[8] For reviews see: a) M. Fujita, *Chem. Soc. Rev.* **1998**, *27*, 417–425; b) C. J. Jones, *Chem. Soc. Rev.* **1998**, *27*, 289–299; c) R. V. Slone, K. D. Benkstein, S. Bélanger, J. T. Hupp, I. A. Guzei, A. L. Rheingold, *Coord. Chem. Rev.* **1998**, *171*, 221–243; d) S. Leininger, B. Olenyuk, P. J. Stang, *Chem. Rev.* **2000**, *100*, 853–908; e) B. J. Holliday, C. A. Mirkin, *Angew. Chem.* **2001**, *113*, 2076–2097; *Angew. Chem. Int. Ed.* **2001**, *40*, 2022–2043; f) S.-S. Sun, A. J. Lees, *Coord. Chem. Rev.* **2002**, *230*, 171–192.

[9] a) V. Balzani, A. Juris, M. Venturi, *Chem. Rev.* **1996**, *96*, 759–833; b) L. Fabbrizzi, M. Licchelli, P. Pallavicini, *Acc. Chem. Res.* **1999**, *32*, 846–853.

[10] a) P. R. Ashton, V. Balzani, O. Kocian, L. Prodi, N. Spencer, J. F. Stoddart, *J. Am. Chem. Soc.* **1998**, *120*, 11190–11191; b) J.-P. Sauvage, *Acc. Chem. Res.* **1998**, *31*, 611–619.

[11] For rotaxanes containing transition metals on the thread components, see: a) H. Ogino, *J. Am. Chem. Soc.* **1981**, *103*, 1303–1304; b) R. S. Wylie, D. H. Macartney, *J. Am. Chem. Soc.* **1992**, *114*, 3136–3138; c) D. Whang, Y.-M. Jeon, J. Heo, K. Kim, *J. Am. Chem. Soc.* **1996**, *118*, 11333–11334; d) S. J. Loeb, J. A. Wisner, *Chem. Commun.* **1998**, 2757–2758; e) K. Chichak, M. C. Walsh, N. R. Branda, *Chem. Commun.* **2000**, 847–848; f) A. D. Shukla, H. C. Bajaj, A. Das, *Angew. Chem.* **2001**, *113*, 460–462; *Angew. Chem. Int. Ed.* **2001**, *40*, 446–448.

[12] a) K.-S. Jeong, J. S. Choi, S.-Y. Chang, H.-Y. Chang, *Angew. Chem.* **2000**, *112*, 1758–1761; *Angew. Chem. Int. Ed.* **2000**, *39*, 1692–1695; b) S.-Y. Chang, J. S. Choi, K.-S. Jeong, *Chem. Eur. J.* **2001**, *7*, 2687–2697.

[13] For systematic studies on the effect of stopper sizes on the kinetic stability of rotaxanes, see: a) M. Asakawa, P. R. Ashton, R. Ballardini, V. Balzani, M. Bělohradský, M. T. Gandolfi, O. Kocian, L. Prodi, F. M. Raymo, J. F. Stoddart, M. Venturi, *J. Am. Chem. Soc.* **1997**, *119*, 302–310; b) P. R. Ashton, I. Baxter, M. C. T. Fyfe, F. M. Raymo, N. Spencer, J. F. Stoddart, A. J. P. White, D. J. Williams, *J. Am. Chem. Soc.* **1998**, *120*, 2297–2307; c) F. M. Raymo, K. N. Houk, J. F. Stoddart, *J. Am. Chem. Soc.* **1998**, *120*, 9318–9322; d) C. Heim, A. Affeld, M. Nieger, F. Vögtle, *Helv. Chim. Acta* **1999**, *82*, 746–759; e) G. M. Hübner, G. Nachtsheim, Q. Y. Li, C. Seel, F. Vögtle, *Angew. Chem.* **2000**, *112*, 1315–1318; *Angew. Chem. Int. Ed.* **2000**, *39*, 1269–1272.

[14] For the charge effect on the kinetic stability of rotaxanes, see: Y. Kawaguchi, A. Harada, *J. Am. Chem. Soc.* **2000**, *122*, 3797–3798.

[15] For self-assembly of zinc porphyrin based rotaxanes, see C. A. Hunter, C. M. R. Low, M. J. Packer, S. E. Spey, J. G. Vinter, M. O. Vysotsky, C. Zonta, *Angew. Chem.* **2001**, *113*, 2750–2754; *Angew. Chem. Int. Ed.* **2001**, *40*, 2678–2682.

[16] For the catenane system with similar concept, see: a) M. Fujita, F. Ibukuro, K. Yamaguchi, K. Ogura, *J. Am. Chem. Soc.* **1995**, *117*, 4175–4176; b) M. Fujita, *Acc. Chem. Res.* **1999**, *32*, 53–61.

[17] a) P. J. Stang, B. Olenyuk, *Acc. Chem. Res.* **1997**, *30*, 502–518; b) L. R. MacGillivray, J. L. Atwood, *Angew. Chem.* **1999**, *111*, 1080–1096; *Angew. Chem. Int. Ed.* **1999**, *38*, 1018–1033; c) G. F. Swiegers, T. J. Malefetse, *Chem. Rev.* **2000**, *100*, 3483–3537; d) G. F. Swiegers, T. J. Malefetse, *Coord. Chem. Rev.* **2002**, *225*, 91–121; e) S. R. Seidel, P. J. Stang, *Acc. Chem. Res.* **2002**, *35*, 972–983.

[18] a) K.-S. Jeong, J. W. Lee, T.-Y. Park, S.-Y. Chang, *Chem. Commun.* **1999**, 2069–2070; for dinuclear analogues of the bead, see: b) K.-S. Jeong, Y. L. Cho, J. U. Song, H.-Y. Chang, M. G. Choi, *J. Am. Chem. Soc.* **1998**, *120*, 10982–10983; c) K.-S. Jeong, Y. L. Cho, S.-Y. Chang, T.-Y. Park, J. U. Song, *J. Org. Chem.* **1999**, *64*, 9459–9466.

[19] a) C. L. Perrin, T. J. Dwyer, *Chem. Rev.* **1990**, *90*, 935–967; b) D. M. Rudkevich, G. Hilmersson, J. Rebek, Jr., *J. Am. Chem. Soc.* **1998**, *120*, 12216–12225; c) F. Hof, C. Nuckolls, S. L. Craig, T. Martín, J. Rebek, Jr., *J. Am. Chem. Soc.* **2000**, *122*, 10991–10996; d) M. Cai, V. Sidorov, Y.-F. Lam, R. A. Flowers, II, J. T. Davis, *Org. Lett.* **2000**, *2*, 1665–1668; e) M. Pons, O. Millet, *Prog. Nucl. Magn. Reson. Spectrosc.* **2001**, *38*, 267–324.

[20] Details for the equation including experimental treatments are described in the Supporting Information. For a similar study, see reference [13a].

[21] a) H. Friebolin, *Basic One- and Two-Dimensional NMR Spectroscopy*, VCH, Weinheim (Germany), **1991**, pp. 269–273; b) A. Affeld, G. M. Hübner, C. Seel, C. A. Schally, *Eur. J. Org. Chem.* **2001**, 2877–2890.

[22] P. J. Stang, D. H. Cao, S. Saito, A. M. Arif, *J. Am. Chem. Soc.* **1995**, *117*, 6273–6283.

[23] R. S. Macomber, *J. Chem. Educ.* **1992**, *69*, 375–378.

Received: November 21, 2002 [F4598]

  0947-6539/03/0907-1541 $ 20.00+.50/0 